

Improvement of Thermal Fringe Projection for Fast and Accurate 3D Shape Measurement of Transparent Objects

Martin Landmann^{1,2}, Henri Speck¹, Jan Till Schmieder^{1,2}, Stefan Heist¹ and Gunther Notni^{1,3}

¹ Fraunhofer Institute for Applied Optics and Precision Engineering IOF, Albert-Einstein-Str. 7, 07745 Jena, German

² Friedrich Schiller University, Institute of Applied Physics, Abbe Center of Photonics, Albert-Einstein-Str. 6, 07745 Jena, Germany

³ Ilmenau University of Technology, Department of Mechanical Engineering, Gustav-Kirchhoff-Platz 2, 98693 Ilmenau, Germany

Abstract Structured light sensors for three-dimensional (3D) shape measurements working in the visible up to the short-wave infrared range have been intensively investigated in the last decades. Reliable measurements require diffuse reflection of the projected patterns. However, this condition is strongly limited or not fulfilled for transparent, translucent, shiny, or absorbing materials. Based on the scanning from heating approach, we have developed a two-step optical method for the measurement of such uncooperative objects. In this contribution, we present a simplified and robust projection technique of a focused single thermal fringe. Due to the irradiation of only locally strongly restricted areas, we obtain considerably higher intensities which enables us to reduce the total measurement time to or even below the second range while increasing the measurement accuracy. We show measurement results of non-opaque surfaces of objects made of a single material as well as of metal objects. Our customizable setup is of interest for quality assurance, bin picking, digitization, and many other areas of applications.

Keywords 3D shape measurement, thermal fringe projection, surface, infrared, transparent

1 Introduction

Structured light sensors for 3D shape measurements working in the visible up to the short-wave infrared range have become more and more important in recent years. Diffuse reflection of the projected patterns is required to obtain reliable results. However, this condition is strongly limited or not fulfilled for transparent, translucent, shiny, or absorbing materials. There have been several approaches [1–3] to measure such uncooperative objects. Based on the scanning from heating approach proposed by Pelletier et al. [4], Eren et al. [5], and Meriaudeau et al. [6], we have developed a two-step method [7–11].

First, multi-fringe thermal patterns are projected onto the measurement object. The object absorbs the energy resulting in a temperature on the surface. In a second step, the stereo recording of the thermal radiation, which is re-emitted by the object surface, takes place. To generate a thermal pattern onto the (object) surface, a metal mask with vertical slits and strips working is used. The mask works like a slide. Basically, this setup can be used to measure the shape of, e.g. transparent glasses. However, both the measurement time, ranging from a few tens of seconds to minutes, and the measurement accuracy are improvable. A big disadvantage is that at least 50% of the incoming intensity is blocked. The envelope irradiance is Gaussian distributed with the consequence that at the horizontal edges of the measurement field, the irradiance drops down to only 28% of the value in the center.

In this contribution, we present a simplified and robust projection approach of a focused single thermal fringe which is quickly scanned over the object surface. The temperature contrast between adjacent dark (cold) and bright (warm) infrared image areas is the key quantity for the thermal 3D measurement quality. The contrast increase during the irradiation period is counteracted by the thermal diffusion within the object material. Due to the irradiation of only locally strongly restricted areas, we obtain considerably higher irradiances than with multi-fringe projection. This enables us to reduce the irradiation period to only a few milliseconds. Within such short irradiation periods, the effect of thermal diffusion is drastically reduced. Simultaneously to the projection, we record the stereo thermal image. In order to measure the entire surface of the object, a galvanometer scanner sequentially shifts the laser sheet to specified positions at which the irradiation and

recording process is repeated. Although we have a higher number of sequential projections, the total measurement time is substantially reduced to or even below the seconds range while increasing the measurement accuracy. We show measurement results of a transparent glass as well as a metal objects. Our customizable design is attractive for quality inspection, bin picking, digitization and many other applications.

2 Setup of MWIR 3D system based on sequential thermal fringe projection

Instead of projecting several two-dimensional patterns as in the multi-fringe projection technique ([10, 11]), we now scan the object surface with a single thermal fringe. The irradiance of this fringe is by factors higher than in our previous setup. To obtain a sufficiently high contrast, the irradiation period can be drastically reduced. Within such short irradiation periods, the effect of thermal diffusion is significantly reduced. A schematic setup of our MWIR 3D system based on the projection of sequential thermal fringes is shown in Fig. 1.1.

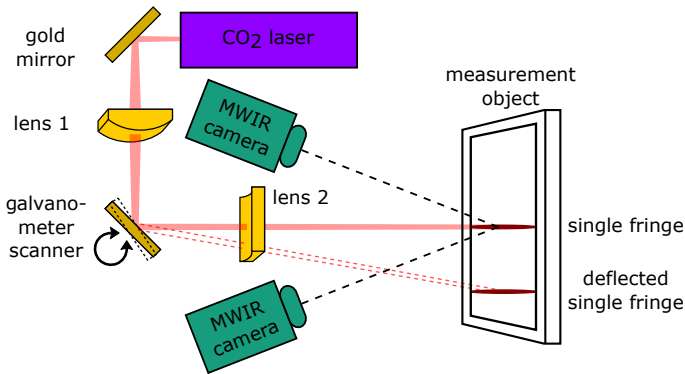


Figure 1.1: Schematic setup of MWIR 3D system based on projection of sequential thermal fringes consisting of projection unit (CO₂ laser, gold mirror, galvanometer scanner, and horizontal ZnSe cylinder lens 1 and vertical ZnSe cylinder lens 2), measurement object, and two MWIR cameras. The projection unit irradiates the measurement object with a single fringe which is sequentially deflected by the galvanometer scanner.

The setup shows two cylindrical ZnSe lenses to transform the CO₂ laser beam into a thin laser line sheet. The convex lens 1 is focusing the beam in horizontal direction while the concave lens 2 is used to irradiate the object in vertical direction. We can adjust the fringe width on the object surface by shifting lens 1 between the gold mirror and the galvanometer scanner or by replacing it with another lens of another focal length. Equivalently, we can move or replace lens 2 to adjust the height of the illuminated measurement field. By changing the beam width or height, the irradiance increases or decreases by the same factor.

The galvanometer scanner enables the sequential horizontal scan of the entire measurement field with the single fringe. The scanning range is flexible and can be adjusted to match the horizontal width of the object. The projected laser line is absorbed by the object and re-emits thermal radiation according to the temperature distribution which we record with two MWIR cameras.

The measurement procedure shown schematically in Fig. 1.2 is similar to the one for the multi-fringe projection setup [12]. The main difference is the significant reduction of the irradiation period. The measurement starts with the first irradiation of a single fringe which lasts for the irradiation period t_{irr} in the milliseconds range. At the same time, both cameras synchronously start to capture the diffused and re-emitted thermal pattern from the object surface. The recording period t_{rec} is the sum of the camera integration time t_{int} and the camera read out time t_{ro} . Immediately after the end of the irradiation period, the galvanometer scanner moves the fringe to the next position (t_{trans}). We set the irradiation period t_{irr} to the maximum (camera recording period t_{rec} minus translation time t_{trans}). For the total measurement time $t_{\text{meas}} = Nt_{\text{rec}}$, the camera frame rate is the limiting factor.

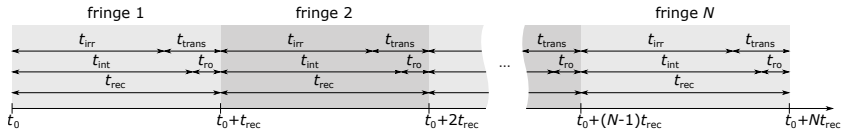


Figure 1.2: Representation of the measurement procedure with sequence length N , irradiation period t_{irr} , translation time t_{trans} , and recording period t_{rec} as the sum of camera integration time t_{int} and the camera read out time t_{ro} .

3 Experimental investigations

After extensive simulation tests with promising results, we designed a laboratory setup according to Fig. 1.1 for the new approach of sequential fringe projection. The distance between the sensor system and the measurement field of $160 \times 128 \text{ mm}^2$ is about 450 mm. The desired vertical width is $w_{\text{ver}} = 120 \text{ mm}$.

With our MWIR 3D system based on sequential fringe projection, we analyzed the 3D result quality dependent on the sequence length N and fringe width w_{hor} . The following results were measured by a recording time of $t_{\text{rec}} = 8 \text{ ms}$. The translation per step took $t_{\text{trans}} = 0.5 \text{ ms}$ and the irradiation period was $t_{\text{irr}} = 7.5 \text{ ms}$. The measurements were conducted on a parallel-sided borosilicate glass plate with a thickness of 3 mm. The determined 3D standard deviation (standard deviation of the 3D points to a fitted plane) refers to an area of $40 \times 40 \text{ mm}^2$.

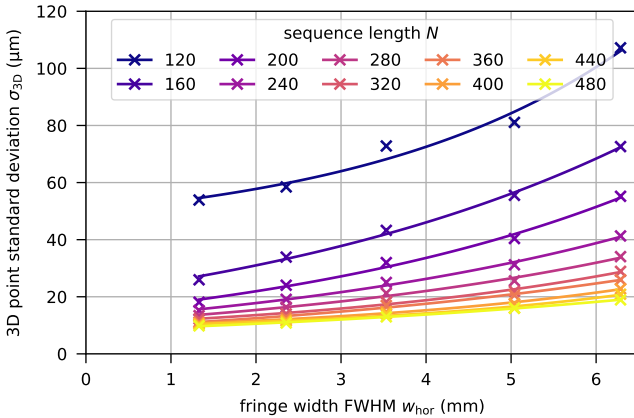


Figure 1.3: 3D point standard deviation σ_{3D} for sequential fringe projection as a function of the horizontal fringe width w_{hor} (1.3 mm...6.2 mm) for different sequence lengths N (120...480) and an integration time of $t_{\text{int}} = 7.8 \text{ ms}$.

Figure 1.3 illustrates the 3D standard deviation as a function of the horizontal fringe width w_{hor} and the sequence length N . The measurements were taken for five different fringe widths (from 1.3 mm to 6.2 mm) for ten different sequence lengths (120...480). These differ-

ent horizontal fringe widths were created by changing the position of the horizontal focus lens or replacing them by another one. With a recording time $t_{\text{rec}} = 8 \text{ ms}$, 120 sequentially projected sequences correspond to a measuring time of 0.96 s. The lowest standard deviation was achieved with the smallest fringe width of 1.3 mm. By increasing the number of fringes per measurement, the measured object is scanned more precisely and more images are used for the 3D result, which results in a smaller standard deviation but in an increased measurement time.

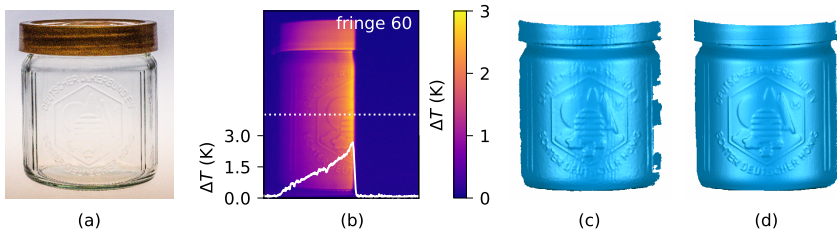


Figure 1.4: 3D measurement example: (a) photograph of a honey jar, (b) left MWIR camera image and temperature profile curve, (c) 3D result for $N = 125$ and $t_{\text{meas}} = 1 \text{ s}$, (d) 3D result for $N = 500$ and $t_{\text{meas}} = 4 \text{ s}$

4 3D measurement example

We measured a honey jar with a plastic cap with $t_{\text{rec}} = 8 \text{ ms}$ ($t_{\text{irr}} = 7.5 \text{ ms}$, $t_{\text{int}} = 7.8 \text{ ms}$), $w_{\text{hor}} = 1.3 \text{ mm}$, and $N = 10 \dots 500$. Figure 1.4 shows the measurement example with a photograph, a typical MWIR camera image as well as an exemplary 3D results for $N = 125$ and $N = 500$. It is already possible to obtain reasonable 3D results with measurement times of just one second (Fig. 1.4(c)). By increasing the sequence length and the measuring time from 1 s to 4 s, the 3D result can be improved considerably (Fig. 1.4(d)). Depending on the application, the setup can optionally measure very accurately (measurement accuracy about $10 \mu\text{m}$) or very quickly (3D acquisition in less than 1 s). In the case of bin picking, short measurement times are required, the contour of the objects must be determined, and details are mostly unimportant. In contrast, in quality assurance, a high mea-

surement accuracy is required. Moreover, objects with metal surfaces (e.g., metal cup, see Fig. 1.5) could also be measured. The previous measurement system based on multi-fringe projection was not able to provide reliable measurement results (Fig.1.5(c)) due to three disadvantages that occur with metallic materials: (1) high reflectivity of projected irradiance, (2) high thermal conductivity, and (3) low emissivity in MWIR.

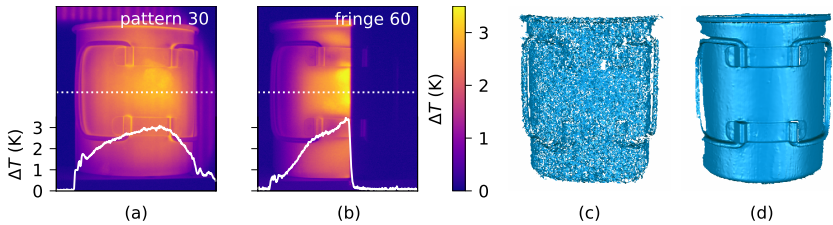


Figure 1.5: 3D measurement example metal cup: (a) left MWIR camera image and temperature profile curve for multi-fringe projection, (b) left camera MWIR image and temperature profile curve for sequential fringe projection, (c) 3D result for $t_{\text{meas}} = 42\text{ s}$ for multi-fringe projection, (d) 3D result for $t_{\text{meas}} = 4\text{ s}$ for sequential fringe projection

5 Improvement of thermal fringe projection

In additions to the improvements due to higher irradiances, the sequential fringe projection with a galvanometer scanner has several advantages over the multi-fringe technique:

1. The first improvement is the strong increase in uniform radiation. In contrast to the multi-fringe technique (at the edges of the measurement field, the irradiance drops down to only 28 % of the value in the center), with the sequential fringe technique we can project an almost homogenous fringe over the entire measurement field (horizontal edges to 98.8 % of the value in the center).
2. By using only a few lenses and mirrors, we (are able to) remove the blocking mask, which absorb at least 50 % of the incoming intensity, and increase the total intensity on the measurement field.

3. Due to the simple flexible structure of the projection system, individual lenses can be moved or exchanged in order to adapt quickly to different conditions like measuring time, accuracy, or different object sizes.
4. The sequential fringes are not imaged onto the measurement object. This makes it easy to vary the distance between the target and the measuring system. By simply shifting the cylindrical lenses, the fringe width and the vertical extension can be modified.
5. With the knowledge of the measurement object geometry, the range of the galvanometer scanner can be changed to decrease measurement time while maintaining the accuracy. If higher measurement accuracy is required in certain areas, the fringe density can be increased by utilizing special algorithms.

6 Conclusion

In this contribution, we presented the new sequential fringe projection system based on the scanning from heating approach. Instead of projecting several two-dimensional patterns, we propose to scan with a single infrared line across the object. After the general system design, we described the measurement procedure. For this new projection system, we only need few components, such as a radiation source for the generation of the heat fringe, some gold mirrors and lenses for shaping and redirecting the laser beam, and a fast turning mirror for scanning over the object. With the resulting thin fringes, we can drastically reduce the irradiation period to a few milliseconds. The previous system based on multi-fringe technique has measuring times ranging from a few tens of seconds to minutes. We presented different parameters and their influences to the measurement quality. An increase in measurement quality can be achieved both by increasing the number of projected fringes and by using very thin fringes.

We also demonstrated the advantages of the sequential fringe technique by objects with high thermal diffusion. The previous measurement system based on multiple fringes was not able to provide reliable measurement results of a metal cup. With the sequential fringe

technique, we are able to measure such objects in significantly shorter time. The experimental studies showed promising results, as not only the measurement accuracy (about $10\ \mu\text{m}$) is increased, but also the measurement time (less than 1 s) is significantly reduced. With these improvements to our system, this measurement technology based on scanning from heating can be applied, e.g., in industrial applications such as quality assurance or bin picking.

For faster measurements, the camera recording time is the limiting factor. In further investigations, the use of high-speed infrared cameras can exceed this limit. Integrating a rotary table into the setup will enable us to perform 360° measurements.

Funding

This research project (2018 FGR 0098, project acronym “3DWÄRME”) is supported by the Free State of Thuringia, the European Social Fund (ESF) of the European Union, and the Thüringer Aufbaubank (TAB).

References

1. I. Ihrke, K. N. Kutulakos, H. P. A. Lensch, M. Magnor, and W. Heidrich, “Transparent and Specular Object Reconstruction,” *Computer Graphics Forum*, vol. 29, no. 8, pp. 2400–2426, 2010. [Online]. Available: <http://dx.doi.org/10.1111/j.1467-8659.2010.01753.x>
2. F. Mériaudeau, R. Rantson, D. Fofi, and C. Stolz, “Review and comparison of non-conventional imaging systems for three-dimensional digitization of transparent objects,” *J. Electron. Imaging*, vol. 21, no. 2, p. 021105, 2012. [Online]. Available: <https://doi.org/10.1117/1.JEI.21.2.021105>
3. S. Lee and H. Shim, “Skewed stereo time-of-flight camera for translucent object imaging,” *Image Vis Comput.*, vol. 43, pp. 27–38, 2015,]. [Online]. Available: <https://doi.org/10.1016/j.imavis.2015.08.001>
4. J.-F. Pelletier and X. Maldague, “Shape from heating: a two-dimensional approach for shape extraction in infrared images,” *Opt. Eng.*, vol. 36, no. 2, pp. 370–375, 1997. [Online]. Available: <https://doi.org/10.1117/1.601210>
5. G. Eren, O. Aubreton, F. Meriaudeau, L. S. Secades, D. Fofi, A. T. Naskali, F. Truchetet, and A. Ercil, “Scanning from heating: 3D shape estimation of transparent objects from local surface heating,” *Opt.*

- Express*, vol. 17, no. 14, pp. 11457–11468, 2009. [Online]. Available: <https://doi.org/10.1364/OE.17.011457>
6. F. Meriaudeau, L. A. S. Secades, G. Eren, A. Erçil, F. Truchetet, O. Aubreton, and D. Fofi, “3-D scanning of nonopaque objects by means of imaging emitted structured infrared patterns,” *IEEE Trans. Instrum. Meas.*, vol. 59, no. 11, pp. 2898–2906, 2010. [Online]. Available: <https://doi.org/10.1109/TIM.2010.2046694>
 7. A. Brahm, C. Rößler, P. Dietrich, S. Heist, P. Kühmstedt, and G. Notni, “Non-destructive 3D shape measurement of transparent and black objects with thermal fringes,” *Proc. SPIE*, vol. 9868, p. 98680C, 2016. [Online]. Available: <http://dx.doi.org/10.1117/12.2227093>
 8. A. Brahm, E. Reetz, S. Schindwolf, M. Correns, P. Kühmstedt, and G. Notni, “3D shape measurement with thermal pattern projection,” *Adv. Opt. Technol.*, vol. 5, no. 5-6, pp. 405–413, 2017. [Online]. Available: <https://www.degruyter.com/view/j/aot.2016.5.issue-5-6/aot-2016-0052/aot-2016-0052.xml>
 9. A. Brahm, S. Schindwolf, M. Landmann, S. Heist, P. Kühmstedt, and G. Notni, “3D shape measurement of glass and transparent plastics with a thermal 3D system in the mid-wave infrared,” *Proc. SPIE*, vol. 10667, p. 106670D, 2018. [Online]. Available: <https://doi.org/10.1117/12.2304777>
 10. M. Landmann, S. Heist, A. Brahm, S. Schindwolf, P. Kühmstedt, and G. Notni, “3D shape measurement by thermal fringe projection: optimization of infrared (IR) projection parameters,” *Proc. SPIE*, vol. 10667, p. 1066704, 2018. [Online]. Available: <https://doi.org/10.1117/12.2304761>
 11. M. Landmann, S. Heist, P. Kühmstedt, and G. Notni, “3D shape from thermal patterns: investigation of projection parameters in simulation and experiment,” *Proc. SPIE*, vol. 11056, p. 1105615, 2019.
 12. M. Landmann, S. Heist, P. Dietrich, H. Speck, P. Kühmstedt, A. Tünnermann, and G. Notni, “3D shape measurement of objects with uncooperative surface by projection of aperiodic thermal patterns in simulation and experiment,” *Opt. Eng.*, vol. 59, no. 9, p. 094107, 2020.